

High-precision measurement of the proton elastic form factor ratio $\mu_p G_E/G_M$ at low Q^2

X. Zhan^{a,b}, K. Allada^c, D. S. Armstrong^d, J. Arrington^b, W. Bertozzi^a,
 W. Boeglin^e, J.-P. Chen^f, K. Chirapatpimol^g, S. Choi^h, E. Chudakov^f,
 E. Cisbani^{i,j}, P. Decowski^k, C. Dutta^c, S. Frullaniⁱ, E. Fuchey^l, F. Garibaldiⁱ,
 S. Gilad^a, R. Gilman^{f,m}, J. Glistner^{n,o}, K. Hafidi^b, B. Hahn^d, J.-O. Hansen^f,
 D. W. Higinbotham^f, T. Holmstrom^p, R. J. Holt^b, J. Huang^a, G. M. Huber^q,
 F. Itard^l, C. W. de Jager^f, X. Jiang^m, M. Johnson^r, J. Katich^d, R. de Leo^s,
 J. J. LeRose^f, R. Lindgren^g, E. Long^t, D. J. Margaziotis^u, S. May-Tal Beck^v,
 D. Meekins^f, R. Michaels^f, B. Moffit^{a,f}, B. E. Norum^g, M. Olson^w,
 E. Piassetzky^x, I. Pomerantz^x, D. Protopopescu^y, X. Qian^z, Y. Qiang^{z,f},
 A. Rakhman^{aa}, R. D. Ransome^{mm}, P. E. Reimer^b, J. Reinhold^e, S. Riordan^g,
 G. Ron^{x,ab}, A. Saha^f, A. J. Sartyⁿ, B. Sawatzky^{f,ac}, E. C. Schulte^{mm},
 M. Shabestari^g, A. Shahinyan^{ad}, R. Shneur^x, S. Širca^{ae,af}, P. Solvignon^{b,f},
 N. F. Sparveris^{a,ac}, S. Strauch^{ag}, R. Subedi^g, V. Sulkosky^{a,f}, I. Vilardi^s,
 Y. Wang^{ah}, B. Wojtsekhowski^f, Z. Ye^{ai}, Y. Zhang^{aj}

^aMassachusetts Institute of Technology, Cambridge, MA 02139, USA

^bPhysics Division, Argonne National Laboratory, Argonne, IL 60439, USA

^cUniversity of Kentucky, Lexington, KY 40506, USA

^dCollege of William and Mary, Williamsburg, VA 23187, USA

^eFlorida International University, Miami, FL 33199, USA

^fThomas Jefferson National Accelerator Facility, Newport News, VA 23606, USA

^gUniversity of Virginia, Charlottesville, VA 22904, USA

^hSeoul National University, Seoul 151-747, Korea

ⁱINFN, Sezione di Roma - Gruppo Sanità, I-00161 Rome, Italy

^jIstituto Superiore di Sanità, I-00161 Rome, Italy

^kSmith College, Northampton, MA 01063, USA

^lUniversité Blaise Pascal, F-63177 Aubiere, France

^mRutgers, The State University of New Jersey, Piscataway, NJ 08855, USA

ⁿSaint Mary's University, Halifax, Nova Scotia, B3H 3C3, Canada

^oDalhousie University, Halifax, Nova Scotia, B3H 3J5, Canada

^pLongwood University, Farmville, VA 23909, USA

^qUniversity of Regina, Regina, SK, S4S 0A2, Canada

^rNorthwestern University, Evanston, IL 60208, USA

^sDipartimento di Fisica and INFN sez. Bari, Bari, Italy

^tKent State University, Kent State, OH 44242, USA

^uCalifornia State University Los Angeles, Los Angeles, CA 90032, USA

^vNRCN, P.O. Box 9001, Beer-Sheva, 84190, Israel

^wSaint Norbert College, De Pere, WI 54115, USA

^xTel Aviv University, Tel Aviv 69978, Israel

^yUniversity of Glasgow, Glasgow G12 8QQ, Scotland, UK

^zDuke University, Durham, NC 27708, USA

^{aa}Syracuse University, Syracuse, NY 13244, USA

^{ab}Lawrence Berkeley National Lab, Berkeley, CA 94720, USA

^{ac}Temple University, Philadelphia, PA 19122, USA

^{ad}Yerevan Physics Institute, Yerevan 375036, Armenia

^{ae}Institute "Jožef Stefan", 1000 Ljubljana, Slovenia

^{af}Dept. of Physics, University of Ljubljana, 1000 Ljubljana, Slovenia

^{ag}University of South Carolina, Columbia, SC 29208, USA

^{ah}University of Illinois at Urbana-Champaign, Urbana, IL 61801, USA

Abstract

We report a new, high-precision measurement of the proton elastic form factor ratio $\mu_p G_E/G_M$ for the four-momentum transfer squared $Q^2 = 0.3\text{--}0.7$ (GeV/c)². The measurement was performed at Jefferson Lab (JLab) in Hall A using recoil polarimetry. With a total uncertainty of approximately 1%, the new data clearly show that the deviation of the ratio $\mu_p G_E/G_M$ from unity observed in previous polarization measurements at high Q^2 continues down to the lowest Q^2 value of this measurement. The updated global fit that includes the new results yields an electric (magnetic) form factor roughly 2% smaller (1% larger) than the previous global fit in this Q^2 range. We obtain new extractions of the proton electric and magnetic radii, which are $\langle r_E^2 \rangle^{1/2} = 0.875 \pm 0.010$ fm and $\langle r_M^2 \rangle^{1/2} = 0.867 \pm 0.020$ fm. The charge radius is consistent with other recent extractions based on the electron-proton interaction, including the atomic hydrogen Lamb shift measurements, which suggests a missing correction in the comparison of measurements of the proton charge radius using electron probes and the recent extraction from the muonic hydrogen Lamb shift.

The nucleon electromagnetic form factors are fundamental quantities which relate to the charge and magnetization distributions within the nucleon. For over 40 years, the form factors have been studied extensively by Rosenbluth separations of the unpolarized electron-proton scattering cross section. Recent advances in the technology of intense polarized beams, polarized targets and polarimetry ushered in a new generation of experiments that measure double polarization observables [1, 2, 3]. Although the proton electric to magnetic form factor ratio $R \equiv \mu_p G_E/G_M$ determined by unpolarized measurements showed minimal Q^2 dependence up to $Q^2 \approx 6$ (GeV/c)², experiments at JLab with high-quality polarized electron beams measuring recoil polarization [4, 5, 6] revealed that the ratio $\mu_p G_E/G_M$ drops almost linearly with Q^2 for $Q^2 > 1$ (GeV/c)². These findings led to an explosion of experimental and theoretical efforts to understand the proton form factors [7, 2, 3]. The difference between the polarization and cross section measurements is now believed to be the result of two-photon exchange (TPE) contributions [8, 9, 10, 11], which have little impact on the polarization measurements but significantly affect the Rosenbluth extractions of G_E at large Q^2 .

While measurements at large momentum transfer have provided information on the fine details of the proton structure and relate to the quark orbital angular momentum, the low Q^2 form factor behavior is sensitive to the long-range structure which is believed to be dominated by the “pion cloud”. High-precision measurements at low Q^2 were motivated by a recent semi-phenomenological

Table 1: Kinematic settings for the experiment. θ_e (θ_p) is the scattered electron (proton) angle in the lab frame, P_p is the proton central momentum, ε is the virtual photon polarization.

Q^2 (GeV/c) ²	θ_e (deg)	θ_p (deg)	P_p (GeV/c)	ε	Analyzer thickness
0.298	28.5	60.0	0.565	0.88	2.25"
0.346	31.3	57.5	0.616	0.85	2.25"
0.402	34.2	55.0	0.668	0.82	3.75"
0.449	36.7	53.0	0.710	0.80	3.75"
0.494	39.2	51.0	0.752	0.78	3.75"
0.547	41.9	49.0	0.794	0.75	3.75"
0.599	44.6	47.0	0.836	0.72	3.75"
0.695	49.8	43.5	0.913	0.66	3.75"

fit [12], which suggested that structure might be present in all four nucleon form factors at $Q^2 \approx 0.3$ (GeV/c)². Later polarization measurements from MIT-Bates [13] and JLab [14] probed this region with a precision of $\sim 2\%$, but found no indication of such structure in the ratio $\mu_p G_E/G_M$.

This Letter reports on a new, high-precision polarization transfer measurement (JLab E08-007) of the proton form factor ratio $\mu_p G_E/G_M$ at Q^2 values between 0.3 and 0.7 (GeV/c)². In the one-photon exchange (Born) formalism, the ratio of the transferred transverse to longitudinal polarizations is related to the proton form factors [2]:

$$R \equiv \mu_p \frac{G_E}{G_M} = -\mu_p \frac{E_e + E'_e}{2M_p} \tan\left(\frac{\theta_e}{2}\right) \frac{P_t}{P_l}, \quad (1)$$

where M_p and μ_p are the proton mass and magnetic moment, E_e (E'_e) is the incident (scattered) electron energy, θ_e is the electron scattering angle and P_t (P_l) is the transverse (longitudinal) component of the polarization transfer.

The experiment was performed at Jefferson Lab in Hall A [15]. A 1.2 GeV polarized electron beam of between 4 and 15 μ A was incident on a 6 cm thick liquid hydrogen target. The beam helicity was changed at 30 Hz, with a quartet structure selected pseudorandomly between (+ - -+) and (- + +-) for each set of four helicity states. The beam polarization was near 83%, as measured by the Møller polarimeter in the Hall [15]. The recoil proton was detected by the left High Resolution Spectrometer (LHRS) in coincidence with the elastically scattered electron detected in a large acceptance spectrometer ("BigBite"). The transferred proton polarization was measured by a focal plane polarimeter (FPP) in the LHRS [15]. The trigger was a coincidence between detection of a charged particle in the HRS and a signal in the BigBite calorimeter used to select energetic electrons. Since elastic events can be well identified using the proton kinematics, only information from the BigBite calorimeter was used in the analysis; the tracking detectors were not turned on for the experiment. The kinematic settings are given in Table 1.

The FPP measured the azimuthal asymmetry due to the spin-orbit coupling in proton scattering from carbon nuclei. The proton's transferred polarization

was extracted by a weighted-sum method [16] based on a COSY [17] model of the spin precession in the spectrometer. Due to the fast reversal of beam helicity, the helicity-independent corrections (acceptance, detector efficiency, target density, etc.) cancel. At each Q^2 value, measurements were taken at the nominal elastic kinematics and with the HRS spectrometer momentum shifted by +2% and -2% to allow for additional systematic studies of the spin transport model. The kinematic factors in Eq. 1 were determined from the beam energy E_e and the proton scattering angle θ_p .

A series of cuts were applied to cleanly select the elastic events and minimize the systematic uncertainties. In addition to the standard HRS cuts (tracking, acceptance, timing, etc.), cuts on the FPP variables were applied to select the events with reliable second-scattering reconstruction [18]. For elastic event selection, we use the correlation between the proton angle and momentum. After applying a tight cut (1.7σ) on the elastic peak and a target vertex cut, the contamination from the aluminum endcaps of the target and neutral pion photoproduction is less than 0.1% in the extracted ratio $\mu_p G_E/G_M$, which is negligible compared to other systematic uncertainties.

The primary systematic uncertainty in the measurement comes from uncertainty in the spin precession of the protons in the spectrometer magnetic fields. The uncertainty arising from imperfect knowledge of the spectrometer fields was estimated by examining the change in the results when key parameters of the spectrometer optics model used for spin precession were altered. The most sensitive parameter is the dipole central bending angle Θ_0 , which is nearly 45° . A conservative 5.5 mrad uncertainty of this parameter is quoted from previous analysis [5], yielding a 0.1–0.6% change in the ratio for different kinematics. In addition, any error in the particle trajectory reconstruction will lead to incorrect proton kinematics at the target which are used as input to the spin precession calculation. The largest effect comes from offsets in the proton angle in the scattering plane, estimated to be ~ 1 mrad based on the consistency of the particle kinematics with the elastic constraint when accounting for the uncertainties of other related parameters (beam energy, proton momentum, spectrometer angle). The associated uncertainty on the extracted form factor ratio is determined to be 0.6–0.9% by manually shifting the proton trajectories in the spin transport [18]. As a final check, the extracted value for $\mu_p G_E/G_M$ was examined as a function of each of the reconstructed proton target variables and for each of the three momentum settings taken for each Q^2 setting. All of these results were consistent within the statistics of the measurements.

The experimental results are summarized in Table 2. The average FPP analyzing power $\langle A_c \rangle$ and efficiency ϵ are in good agreement with previous measurements [19]. When a transversely polarized proton interacts with the FPP, the azimuthal asymmetry induced by the secondary scattering is proportional to the proton polarization and the analyzing power, which depends on the proton momentum and the angle of the secondary scattering. The average analyzing power extracted in the analysis is the event-weighted average over the 5 – 25° range of angles used in the analysis of the experiment. The FPP figure of merit (FOM) is an integral of ϵA_c^2 over the selected θ range. No correction was ap-

Table 2: Experimental ratio $\mu_p G_E/G_M \pm stat. \pm syst.$ along with the average FPP analyzing power $\langle A_c \rangle$, efficiency ϵ and the figure of merit (ϵA_c^2) for secondary scattering angles between 5° and 25° .

Q^2 (GeV/c) ²	$\langle A_c \rangle$	ϵ [%]	FOM [%]	$\mu_p G_E/G_M$
0.298	0.219	5.30	0.25	0.9272±0.0114±0.0071
0.346	0.394	3.67	0.57	0.9433±0.0088±0.0093
0.402	0.466	4.36	0.95	0.9318±0.0066±0.0076
0.449	0.488	4.09	0.97	0.9314±0.0060±0.0073
0.494	0.466	3.81	0.83	0.9286±0.0054±0.0076
0.547	0.430	4.34	0.81	0.9274±0.0055±0.0071
0.599	0.392	4.41	0.68	0.9084±0.0053±0.0104
0.695	0.334	4.74	0.53	0.9122±0.0045±0.0107

plied for two-photon exchange, which is less than a 0.1% correction on P_t/P_l (or G_E/G_M) for these kinematics [9].

With the unprecedented statistical precision, we were able observe a small cut dependence in the analysis when loose cuts (larger than 2σ) were placed on the elastic peak, and so used tighter cuts (1.7σ) than previous experiments where were statistics limited. This also led to a detailed reanalysis of a previous experiment [14], which found that their sensitivity to these effects were small but yielded an improved isolation and correction for events involving scattering from the cryotarget endcaps that led to a slight decrease in the extracted form factor ratio [20].

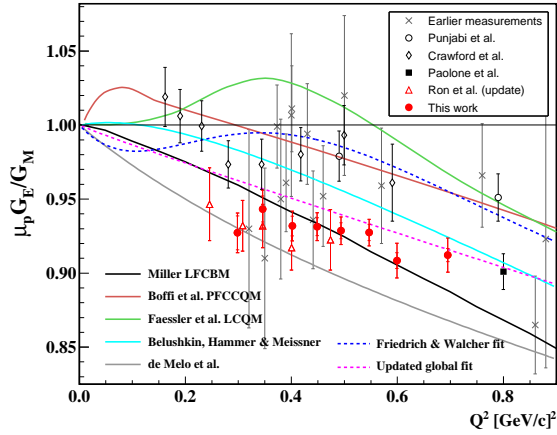


Figure 1: Low Q^2 polarization measurements of $\mu_p G_E/G_M$. The solid red circles are results from E08-007 and the hollow symbols are from previous measurements [5, 13, 20, 21] with precision of better than 3%. The grey crosses show various lower precision data [22, 23, 24, 25]. The solid curves are selected theoretical models of the proton form factors [26, 27, 28, 29, 30]. The dashed curves are the Friedrich and Walcher fit [12], and the updated global fit (see text).

Figure 1 presents the new results together with previous polarization measurements, including the updated results from Ron, *et al* [20]. The inner error bars are the statistical uncertainty and the outer error bars are the statistical and systematic uncertainties added in quadrature. The new results achieved a total uncertainty of $\sim 1\%$, usually dominated by the systematic uncertainties. The data fall slowly across the covered Q^2 range and strongly deviate from unity. The high-precision point at $Q^2 = 0.8$ (GeV/c) 2 [21] is also consistent with the trend of our new results. Compared to the Bates measurement [13], these new ratio results are lower by $2\text{--}3\sigma$, indicating some systematic discrepancy.

Two implications of the new data can be directly seen. Some previous measurements suggested that the ratio was flat at $\mu_p G_E/G_M \approx 1$ until $Q^2 \approx 0.2$ (GeV/c) 2 and then began to fall, which implied identical low- Q^2 behavior of the form factors and thus equal charge and magnetization radii for the proton. We observe that $\mu_p G_E/G_M$ is significantly below one over the entire Q^2 range of our data, with no indication that the ratio is approaching unity noticeably above $Q^2 = 0$. The global fit (described later) suggests that the ratio begins to fall starting at or very near $Q^2 = 0$, implying significant differences in the large scale spatial distribution of charge and magnetization in the proton. Second, with this high precision data, we see no indication of any structure in the ratio $\mu_p G_E/G_M$ over the covered Q^2 region.

The curves in Fig. 1 show a selection of modern fits and models in the literature: a light-front cloudy-bag model (Miller [26]), a point-form chiral constituent quark model (Boffi *et al.* [27]), a Lorentz covariant constituent quark model (Faessler *et al.* [28]), and two representative vector-meson dominance models (Belushkin *et al.* [29] and de Melo *et al.* [30]). None of the existing models precisely match the new results, but we note that despite utilizing different theoretical frameworks, both the calculation of Miller and of de Melo *et al.* are in qualitatively good agreement with our results. As both of these consider the role of non-valence contributions, e.g. nucleon plus pion contributions in addition to the lowest 3-quark Fock state, this provides additional support for the important role of the pion cloud at low Q^2 , even though no structure is seen in this ratio (or in the global fit for G_E and G_M).

We have performed an updated global fit of the form factors, following the procedure of Ref. [31]. In addition to the data sets included in that analysis, we add our new results along with other recent polarization measurements [6, 20, 21], but have not included the more recent cross section measurements from Mainz [32], as these data do not include sufficient information on the uncertainties to be included in a consistent fashion. Figure 2 presents G_E and G_M normalized by the standard dipole form, $G_D = 1/[1 + Q^2/0.71(\text{GeV}/c)^2]^2$, for the previous global fit and our updated fit, along with the Rosenbluth separation value for the cross section analysis of Ref. [31] without the inclusion of TPE corrections. The difference between the cross section analysis (hollow circles) and the global fit (dotted curve), both from Ref. [31], is due to a combination of the TPE corrections and the inclusion of the limited polarization data available at the time. The difference between the dotted curve and our updated fit (solid red curve) comes from the inclusion of the new polarization

data (Refs. [21, 20] and this work). For $0.2 < Q^2 < 1.0$ (GeV/c)², the updated global fit shows a 2% decrease in G_E and a 1% increase in G_M compared to the earlier fit [31]. The inclusion of these precise polarization data also improves the determination of the relative normalization of the different cross section data sets included in the fit, which has a significant impact on the uncertainty in the extraction of the proton charge radius [33].

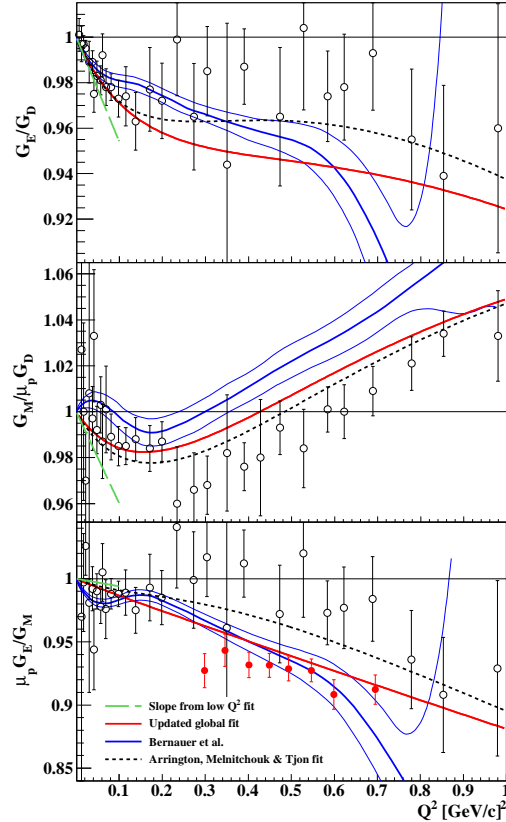


Figure 2: Global fits to G_E , G_M and ratio $\mu_p G_E/G_M$ from ref. [31] (dotted line) and this work (solid red line). The blue lines are the best fit and uncertainty band from the Mainz cross section data [32]. The solid circles are our new results for $\mu_p G_E/G_M$ and the hollow circles show the global cross section analysis of Ref. [31], which do *not* include TPE TPE corrections. The green long-dashed line shows the first term of our low- Q^2 fit used to extract the radius.

We also show the fit to recent Mainz cross section measurements [32] in Fig. 2. The Mainz fit is in reasonable agreement with our direct extraction of $\mu_p G_E/G_M$, but their results for G_E and especially G_M are somewhat inconsistent with our global fit (and systematically above all previous extractions of G_M). However, it is difficult to make a detailed comparison of the results due to differences in TPE corrections. The hollow points do not include any TPE

correction, the global fits include the full TPE corrections of Ref. [9] to the cross sections, while the Mainz extraction [32] applies only the $Q^2 = 0$ limit of the Coulomb distortion correction [34]. This yields an overestimate of the correction at all finite Q^2 values and neglects the Q^2 dependence of the correction which will change the extracted magnetic form factor and magnetic radius [35, 36, 20], but has a much smaller impact on the very low Q^2 behavior of G_E and the extracted charge radius. A full examination of the consistency between the Mainz result and other cross section measurements would require careful examination of the TPE corrections applied to the different data sets and is beyond the scope of the present work.

The proton electric and magnetic RMS radii can be determined from the form factor slope at $Q^2 = 0$:

$$\langle r_{E/M}^2 \rangle = -\frac{6}{G_{E/M}(0)} \left(\frac{dG_{E/M}(Q^2)}{dQ^2} \right)_{Q^2=0}. \quad (2)$$

We do not use the previously described global fit to extract the radius because such fits are dominated by high- Q^2 data which have essentially no sensitivity to the radius. To extract the radius, we repeat the global fit described above using a continued fraction [33] parameterization with fewer parameters, including only cross section and polarization data below $Q^2=0.5$ (GeV/ c)². The radius values we obtain are:

$$\langle r_E^2 \rangle^{1/2} = 0.875 \pm 0.008_{\text{exp}} \pm 0.006_{\text{fit}} \text{ fm} \quad (3)$$

$$\langle r_M^2 \rangle^{1/2} = 0.867 \pm 0.009_{\text{exp}} \pm 0.018_{\text{fit}} \text{ fm}, \quad (4)$$

where the quoted values are the averages from fits with 3, 4, and 5 parameters, the first uncertainty is the result of the experimental uncertainties (statistical, systematic and normalization uncertainties added in quadrature) and the second is the model dependence estimated by taking the scatter of fits when we vary the functional form, number of fitting parameters, and Q^2 cutoff. The slope corresponding to first term of the low- Q^2 analysis is shown in Fig. 2. For G_E , the global fit and low- Q^2 fit are in good agreement as $Q^2 \rightarrow 0$, although by $Q^2 = 0.1$, the higher-order terms are beginning to yield a deviation from the linear term. For G_M , even the slope at $Q^2 = 0$ is slightly different. Because the cross section becomes more sensitive to G_M as Q^2 increases, fits that include high Q^2 data will tend to overemphasize agreement at high Q^2 values at the cost of the low Q^2 behavior. This is why the global fits are generally not well suited to extraction of the radii, especially when fitting the magnetic form factor.

While the charge and magnetic radii yield consistent values, as one would expect in the non-relativistic limit where the quarks carry both the charge and magnetization, the fit yields a different detailed behavior of the form factors even at low Q^2 . This implies a different shape for the charge and magnetization distributions, even though the radii are consistent. If a fixed functional form is chosen for both the charge and magnetic form factors at low Q^2 , the fits yield different radii.

Our magnetic radius is significantly larger than the Mainz value [32]: $\langle r_M^2 \rangle^{1/2} = 0.777 \pm 0.017$ fm. As noted previously, the Coulomb correction applied in that analysis does not include any Q^2 dependence, which will likely lead to an error in the extracted magnetic radius. An analysis of their data with a modern correction for Coulomb distortion (or full two-photon exchange) is required to determine if this represents a true discrepancy between the Mainz result and all other extractions. An initial evaluation [35, 36], using a calculation for the TPE corrections valid up to $Q^2 \approx 1.0$ GeV², yields an increase in the magnetic radius of 0.026 fm, accounting for roughly one-third of the discrepancy.

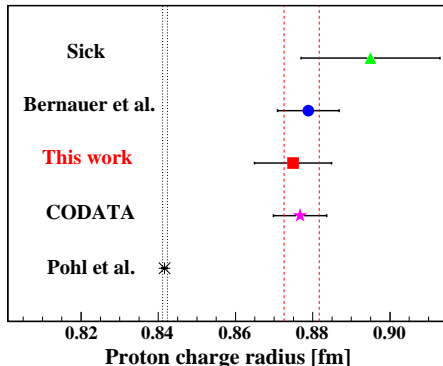


Figure 3: The proton RMS charge radius from a previous ep scattering analysis (Sick [33]), the Mainz low- Q^2 measurement (Bernauer *et al.* [32]) and this work compared to the CODATA [37] and muonic hydrogen spectroscopy (Pohl *et al.* [38]). The red dashed lines show the combined results from CODATA, Bernauer *et al.* and this work while the black dotted lines show the Pohl *et al.* uncertainty.

Several extractions of the proton charge radius are summarized in Fig. 3. Based on totally different data sets, the charge radius extracted here is in excellent agreement with the Mainz extraction 0.879 ± 0.008 fm [32] and the CODATA value 0.8768 ± 0.0069 fm [37], which is mainly inferred from atomic hydrogen spectroscopy. The combined result of the three measurements based on electron-proton interactions gives:

$$\langle r_E^2 \rangle_{ep}^{1/2} = 0.8772 \pm 0.0046 \text{ fm}. \quad (5)$$

The Sick result is shown for comparison but not included in the average because our updated extraction includes all of the data included in Ref. [33]. A recent measurement of the Lamb shift in muonic hydrogen [38] yields a proton charge radius of 0.8418 ± 0.0007 fm, which is 7.7σ from the combined result of the ep measurements. Barring an error in the extraction of the muonic hydrogen result or a common offset affecting both electron scattering and atomic hydrogen measurements, there appears to be a true difference between electron-based and muon-based measurements. This would seem to disfavor explanations that

would lower the CODATA result, e.g. based on a modified value of the Rydberg constant, and suggests a missing correction that differs for electron and muon probes. One mechanism that could cause such a difference was recently proposed [39]. However, there is still significant activity aimed at determining whether the discrepancy is the result of a missing element in the QED corrections in the bound μp system [40] or if a more exotic explanation is required.

In conclusion, we present a new set of high precision form factor ratios extracted using the recoil polarization technique. These data provide improved sensitivity to G_M at low Q^2 while minimizing two-photon exchange corrections which are of particular importance in separating G_E and G_M . Our results have been combined with previous cross section and polarization measurements to provide an improved global analysis of the form factors. The new data shift the extracted values of G_E and G_M at low Q^2 , which will impact the proton structure corrections to atomic energy levels in hydrogen and muonic hydrogen as well as the extraction of the strange quark contribution to the form factors probed in parity-violation ep scattering [41, 42]. While the updated form factors yield only a small modification to the expected parity-violating asymmetry, typically less than half of the assumed uncertainty, it will have a correlated effect on the analysis of all such measurements. Finally, we present an improved extraction of the proton charge and magnetization radii, and find consistency between electron-based probes of the proton radius, which disagree with the muonic hydrogen result.

We thank the Jefferson Lab Physics and Accelerator Divisions. This work was supported by the National Science Foundation, the Department of Energy, including Contract No. DE-AC02-06CH11357, and the US-Israeli Bi-National Scientific Foundation. Jefferson Science Associates operates the Thomas Jefferson National Accelerator Facility under DOE Contract No. DE-AC05-06OR23177.

References

- [1] J. Arrington, C. D. Roberts, J. M. Zanotti, J. Phys. G34 (2007) S23.
- [2] C. F. Perdrisat, V. Punjabi, M. Vanderhaeghen, Prog. Part. Nucl. Phys. 59 (2007) 694.
- [3] J. Arrington, K. de Jager, C. F. Perdrisat, J.Phys.Conf.Ser. 299 (2011) 012002.
- [4] O. Gayou, et al., Phys. Rev. Lett. 88 (2002) 092301.
- [5] V. Punjabi, et al., Phys. Rev. C 71 (2005) 055202. Erratum-ibid. C 71, (2005) 069902.
- [6] A. J. R. Puckett, et al., Phys. Rev. Lett. 104 (2010) 242301.
- [7] I. A. Qattan, et al., Phys. Rev. Lett. 94 (2005) 142301.
- [8] P. A. M. Guichon, M. Vanderhaeghen, Phys. Rev. Lett. 91 (2003) 142303.

- [9] P. G. Blunden, W. Melnitchouk, J. A. Tjon, Phys. Rev. Lett. 91 (2003) 142304.
- [10] Y. C. Chen, A. Afanasev, S. J. Brodsky, C. E. Carlson, M. Vanderhaeghen, Phys. Rev. Lett. 93 (2004) 122301.
- [11] J. Arrington, P. G. Blunden, W. Melnitchouk (2011). ArXiv:1105.0951.
- [12] J. Friedrich, T. Walcher, Eur. Phys. J. A17 (2003) 607.
- [13] C. B. Crawford, et al., Phys. Rev. Lett. 98 (2007) 052301.
- [14] G. Ron, et al., Phys. Rev. Lett. 99 (2007) 202002.
- [15] J. Alcorn, et al., Nucl. Instrum. Meth. A522 (2004) 294.
- [16] D. Besset, et al., Nucl. Instrum. Meth. 166 (1979) 515.
- [17] K. Makino, B. Berz, Nucl. Instrum. Meth. A654 (1999).
- [18] X. Zhan, Ph.D. thesis, Massachusetts Institute of Technology, 2010. ArXiv:1108.4441.
- [19] J. Glister, et al., Nucl. Instrum. Meth. A606 (2009) 578.
- [20] G. Ron, et al. (2011). ArXiv:1103.5784.
- [21] M. Paolone, et al., Phys. Rev. Lett. 105 (2010) 072001.
- [22] B. D. Milbrath, et al., Phys. Rev. Lett. 80 (1998) 452.
- [23] T. Pospischil, et al., Eur. Phys. J. A12 (2001) 125.
- [24] S. Dieterich, et al., Phys. Lett. B500 (2001) 47.
- [25] O. Gayou, et al., Phys. Rev. C 64 (2001) 038202.
- [26] G. A. Miller, M. R. Frank, Phys. Rev. C 65 (2002) 065205.
- [27] S. Boffi, et al., Eur. Phys. J. A14 (2002) 17.
- [28] A. Faessler, T. Gutsche, V. E. Lyubovitskij, K. Pumsa-ard, Phys. Rev. D 73 (2006) 114021.
- [29] M. A. Belushkin, H. W. Hammer, U. G. Meissner, Phys. Rev. C 75 (2007) 035202.
- [30] J. P. B. C. de Melo, T. Frederico, E. Pace, S. Pisano, G. Salme, Phys. Lett. B671 (2009) 153.
- [31] J. Arrington, W. Melnitchouk, J. A. Tjon, Phys. Rev. C76 (2007) 035205.
- [32] J. C. Bernauer, et al., Phys. Rev. Lett. 105 (2010) 242001.

- [33] I. Sick, Phys. Lett. B 576 (2003) 62.
- [34] W. A. McKinley, H. Feshbach, Phys. Rev. 74 (1948) 1759.
- [35] J. Arrington (2011). ArXiv:1008.3058, to appear in Phys.Rev.Lett.
- [36] J. C. Bernauer, et al. (2011). ArXiv:1108.3533.
- [37] P. J. Mohr, B. N. Taylor, D. B. Newell, Rev. Mod. Phys. 80 (2008) 633.
- [38] R. Pohl, et al., Nature 466 (2010) 213.
- [39] G. Miller, A. Thomas, J. Carroll, J. Rafelski (2011). ArXiv:1101.4073.
- [40] U. Jentschura, Eur.Phys.J. D61 (2011) 7.
- [41] R. D. Young, J. Roche, R. D. Carlini, A. W. Thomas, Phys.Rev.Lett. 97 (2006) 102002.
- [42] J. Liu, R. D. McKeown, M. J. Ramsey-Musolf, Phys. Rev. C76 (2007) 025202.